JOURNAL OF ZANKOY SULAIMANI

AUTHOR'S COPY

Part -A- (Pure and Applied Sciences)
VOLUME 25 ISSUE 2 December 2023
ISSN: 1812-4100
www.jzs.univsul.edu.iq

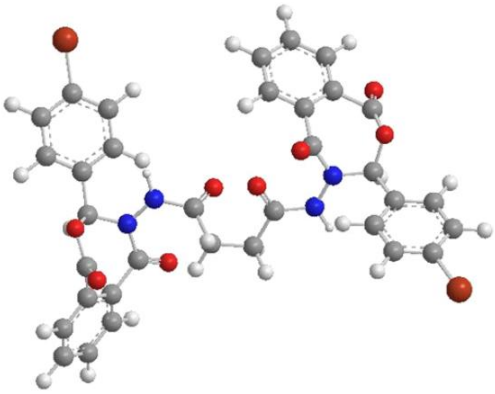

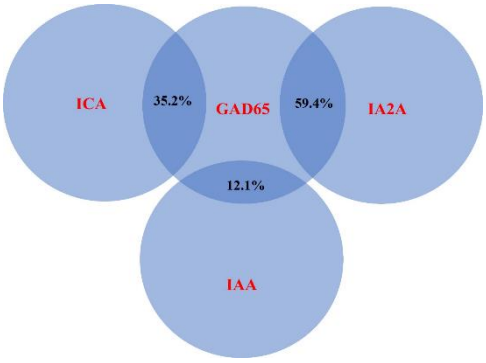

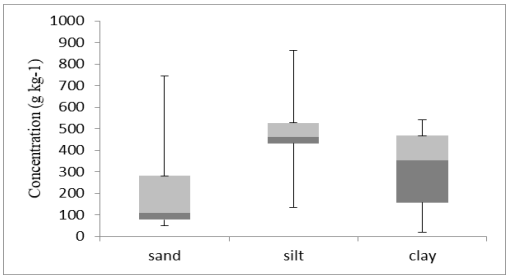

Journal homepage www.jzs.univsul.edu.iq
Journal of Zankoy Sulaimani
Part-A- (Pure and Applied Sciences)
ISSN:1812-4100

Kinetics, thermodynamics, and DFT studies of phenols oxidative coupling reactions with 4-amino-N, N-dimethylaniline

Sirwan A. Ahmad*, Mohammad T. Kareem

Department of Chemistry, College of Science, University of Sulaimani, 46001 Sulaymaniyah, Kurdistan, Iraq
*Correspondence: sirwan.abdalla@univsul.edu.iq

Article info

Original: 13/05/2023
Revised: 25/07/2023
Accepted: 14/08/2023
Published online: 20/12/2023

Key Words:
Oxidative coupling reaction, Phenol, Stability constant, Rate constants, Thermodynamic parameters

Abstract

A spectrophotometric method has been established for the reaction kinetics of phenol oxidative coupling with 4-amino-N, N-dimethylaniline in the presence of potassium dichromate as an oxidant to form $C_{14}H_{14}N_2O$, known as phenol blue. Optimum conditions for the reaction were investigated: maximum wavelength (λ max), linear range, molar absorbtivity, and stability constant. The kinetic models were applied to the reaction, indicating that it is a first-order reaction. The activation energy (Ea) and Arrhenius constant (A) were calculated from the Arrhenius equation as 14.89 kJ·mol^{-1} and 3.75 × 10^5 s^{-1} respectively. Thermodynamic parameters were ΔH* 12.37 Kj·mol^{-1}, ΔG* 5.47 kJ·mol^{-1} and ΔS* 22.77 J·mol^{-1}·K^{-1} at 30°C.. Results indicate that the formation of the product phenol blue is non-spontaneous and endothermic in nature. Density function theory (DFT) has been done for the comparison between experimental and theoretical results using the common 6-311G(d,p) basis set. The results are in good agreement with each other, proving the reliability of the method.Finally,some preliminary test has been performed to check possibility of the product as dye.

Introduction

Oxidative coupling is a promising alternative to cross-coupling that may address concerns regarding substrate functionalization and electropositive atoms connected to nucleophilic carbon. In oxidative processes, two nucleophilic centers, such as carbon, oxygen, nitrogen, or another kind, are coupled. Although cross-coupling and oxidative coupling have many practical differences, they share a similar fundamental structure. Pre-functionalization is often not required in oxidative coupling since the nucleophilic centers are frequently bound to hydrogen and the reaction requires an external (or internal) oxidant to remain electroneutral (1).

The mechanism of the cross-coupling catalytic cycle consists of three main phases: oxidative addition, transmetallation, and reductive elimination (2). Phenols and their derivatives are the fundamental building blocks for various types of complex compounds essential to the functioning of biological systems. Phenol-phenol oxidative coupling reactions involve a variety of processes, but with well-researched catalysts, the reaction outcomes can be predicted quite accurately (3). Sequential couplings provide access to oligomers and polymers with clearly defined structural properties. Iron(III) chloride is readily available and reasonably priced

for commercial use; it is a popular oxidant for the oxidative C-C coupling of arenes and related unsaturated molecules. The method enables highly selective dimerizations of heterocyclic compounds, naphthols, and derivatives of phenol (4). Oxidation of phenols generates phenoxy radicals, which couple with little selectivity to form C-C and C-O bonds primarily at the ortho and para positions of the phenolic hydroxyl.

Several oxidants have been used for phenol oxidative coupling, such as selenoxide, which is a selective oxidant for intramolecular coupling between phenol and catechol, and silver oxide (Ag_2O), which is used as a chemical oxidant in the oxidative cross-coupling of p-hydroxycinnamic alcohols (5,6). The selective $FeCl_3$-catalyzed oxidative cross-coupling reaction between phenols and primary, secondary, and tertiary 2-amino naphthalene derivatives has been investigated (7). However, it is challenging and rarely accomplished to create selective oxidative cross-coupling reactions between phenols and unprotected anilines (8). Peroxidase mimics, such as Schiff base complexes (9) and metal-phthalocyanines, have been applied to the determination of H_2O_2 and phenol in clinical chemical analysis and to the oxidative coupling of 2,6-dimethylphenol (10,11).

The study of kinetic techniques involves measuring the progress of reactions across a wide range of scales, from chemical bond interactions between atoms and electrons to chemical production rates in reactors. Kinetic approaches have numerous advantages, including high selectivity methods that assess absorbance as a function of reaction time rather than a specific absorbance value (12). They also provide simple and fast procedures, skipping several experimental stages such as filtration and extraction before absorbance measurements. However, there is a lack of physical assay techniques based on oxidative phenol coupling kinetics in the literature. Although Brooker synthesized phenol blue as a unionized dye, the reaction kinetics have not been studied to date (13). This investigation aims to describe the oxidation of phenol with 4-amino-N N-dimethylaniline to produce blue phenol in an alkaline medium with the determination of kinetics and thermodynamics parameters, of activation.

Materials and Methods

Materials

Phenol, C_6H_6O (94.11 g/mol, purity 99%), potassium dichromate $K_2Cr_2O_7$ (294.18 g/mol) were purchased from Sigma-Aldrich, 4-amino-N, N-dimethylaniline chloride(208.15 g/mol) (purity 97% was purchased from Fluka, and sodium hydroxide pellets (40.00 g/mol) purchased from Merck. All the chemical reagents were used without further purification. All reactant solutions must be kept inside a heating-cooling water bath at the required temperature for thermal equilibration.

Preparation of stock solutions:

A stock solution of 1000 mg/L of phenol was prepared by dissolving 0.1 g in 100 ml of distilled water, followed by a series of concentrations (20, 40, 60, 80, and 100 mg/L) by dilution with distilled water. Stock solution of 1000 mg/L of a reagent, 4-amino-N, N-dimethylaniline, has been prepared by dissolving 0.1 g in 100 ml of distilled water. The oxidant substance potassium dichromate (0.01 mol/L) was prepared by dissolving 0.367 g in 100 mL distilled water. Finally, the alkaline medium has been prepared by dissolving 0.4 g of NaOH in 100 ml of distilled water.

Study of wave length:

By scanning the wavelength against absorbance between 280 and 780 nm, the wavelength of the product was studied, and the highest wavelength was found to be 665 nm in comparison to the reaction's blank.

The linear range and Molar extinction coefficient of the product:

linear range used to determine linearity range of product , the result show a linear range between (30 -100) mg/L. Molar extinction coefficient of the product was sudied to estimate the sensitivity of the method.

Stability constant:

To show stability of the compound this study has been performed, which is ranging between (14.36 - 20.26)L/mol , the stubility was followed by taking (A) at different periods:(2,4,6,12,24,48,72)hours , the stubility was constant within that times.

Optimization of kinetic experimental conditions:

To get optimum condition(maximum absorbance) , the amounts of (reagent, oxidant and medium) were changed to get such condition . The reactants , including the sample, reagent, oxidant, medium and distilled water were placed in a water bath at the desired temperature. 0.71 ml of phenol samples of all concentrations at different temperatures were added to the cell quartz cell ,with 0.6 ml of NaOH, 0.71 ml of the reagent, and 0.3 ml of potassium dichromate , the total volume was completed to 4 ml(capacity of the cell) by distilled water, and the mixture was quickly mixed in a quartz cuvette. Subsequently, the prepared mixtures were placed in the uv-visible spectrophotometer the absorbance was followed up at different systematic cycle times until constant absorbance.

This is one of the typical time-resolved absorbance peak as output of the computarized spectrophotometer.

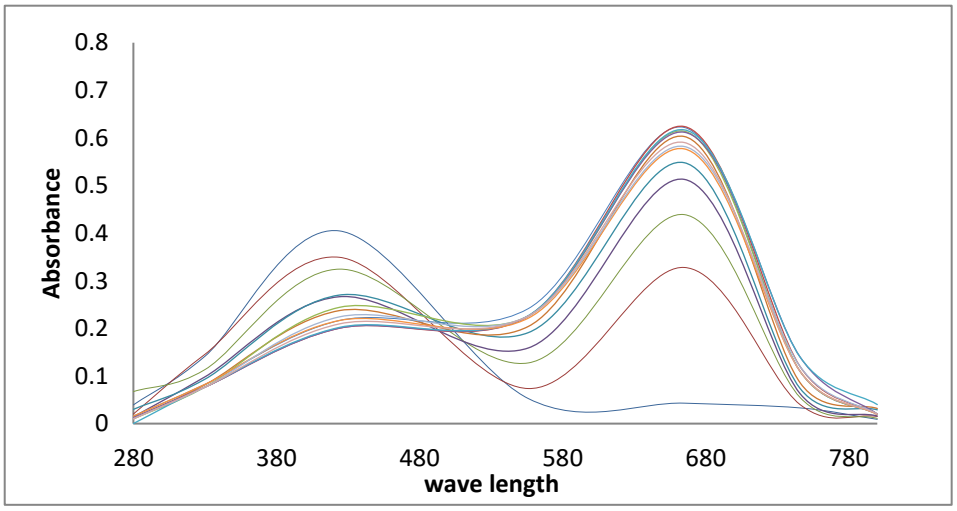

Figure 1: Time – resolved absorption spectra of 60 ppm phenol reaction at 30°C at the cycle time of (6 minutes)

Computational process method;

DFT computations with the common 6-311G(d,p) basis set, Gaussian 09 thermochemistry was employed by inputting all structures of reactants and product to calculate the enthalpy, Gibbs free energy, heat of formation, and absolute reaction rate of the reaction. To compaer the theoritical results with those of the practical.

Dyeing process method

A suitable amount of phenol blue about 0.1g was dissolved in about10 ml of distilled water and (0.1-0.2)g of alum was added as a fixer. A piece of tissues(Cotton,Polyster,Wool) were dipped in the solution and heated to boiling with stirring within few minutes. The tissues were taken out and washed with tap water, followed by hot water with detergent; the stain was fixed on the tissue, indicating that the product may be used as dying material.

Results and Discussion

Preparation of the product

The reaction between phenol and 4-amino-N, N-dimethylaniline with some physical properties :

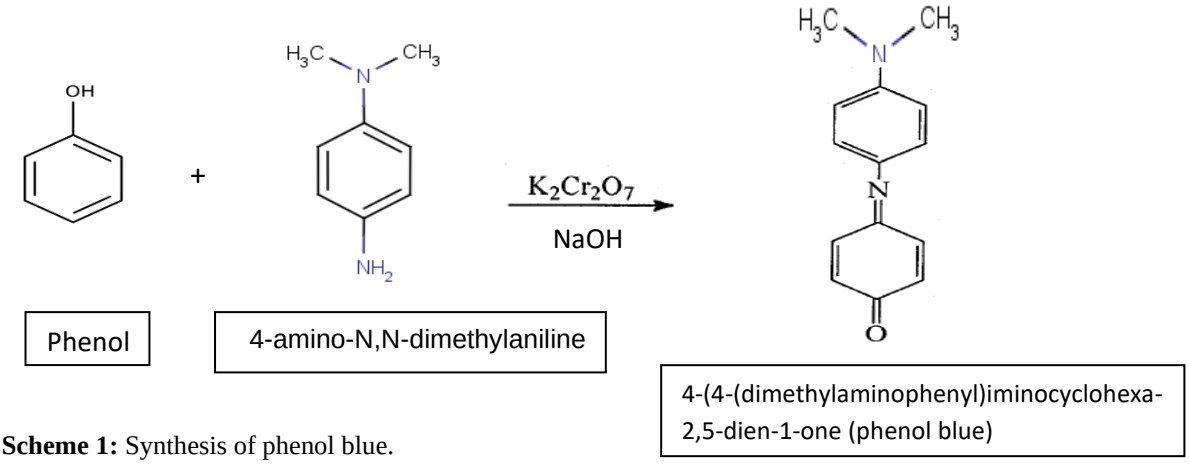

Scheme 1: Synthesis of phenol blue.

Table 1: Some physical properties of blue phenol

Molecular formula	$C_{14}H_{14}N_2O$
Molecular weight	226.27
Melting point	136- 137 ^oC
Boiling point	367
Density	1.085
Maximum wavelength	650 nm
Molar extinction coefficient	1486 $M^{-1}cm^{-1}$

Investigation of the wavelength of the product:

The wavelength of the product has been investigated by scanning the wavelength against absorbance between (280 – 780)nm, and the maximum wavelength was determined at 665 nm compared with the blank of the reaction as shown in Figure 2.

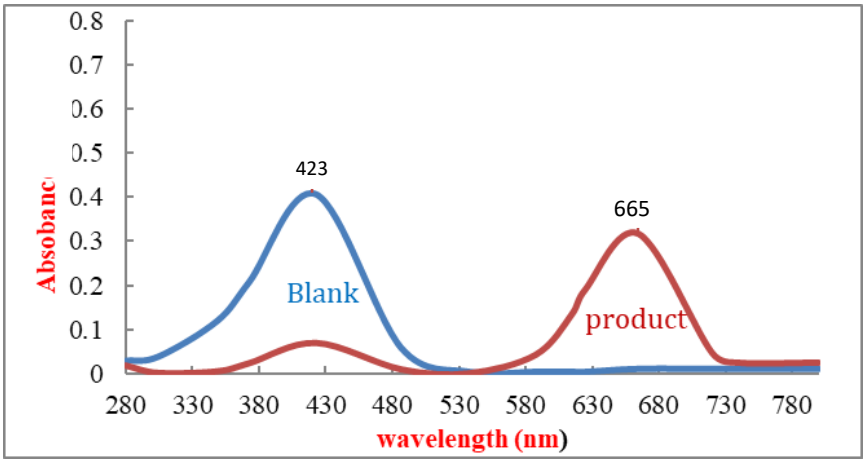

Figure 2: The wavelength of the product

The linear range of the reaction:

Various concentrations of phenol from (20,30,40,50,60,70,80,90,100,110,120)mg/Lwere prepared by serial dilution, suitable amounts of the medium,reagent and oxidant were added to the volumetric flask . The volume was completed to the mark with distilled water, the mixtures were standed for more than 1 hour . the absorbance was measured , and the calibration gragh was constracted the results show a linear range between (30 -100) mg/L, as in the Figure 3.

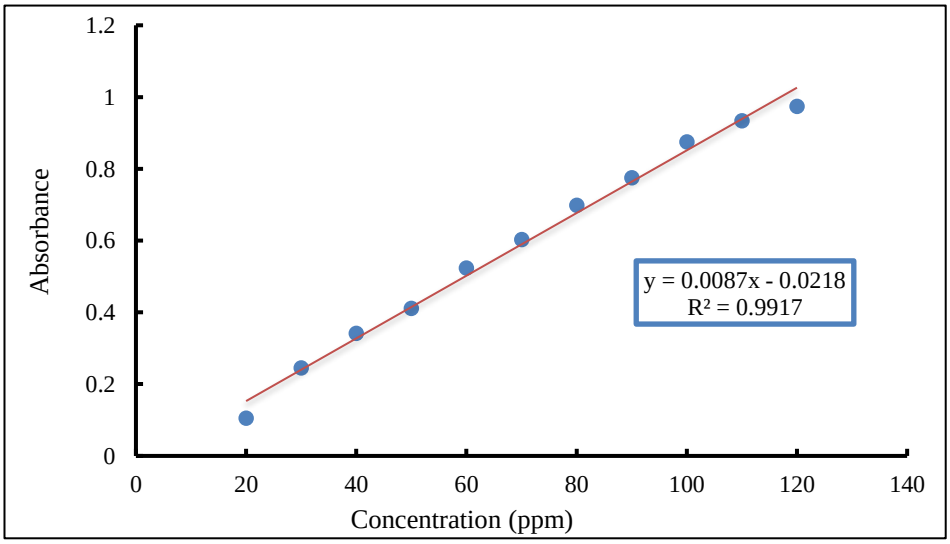

Figure 3: Linear range study of the reaction.

Determination of the molar extinction coefficient of the product:

The reaction of phenol with 4-amino-N, N-dimethylaniline in the presence of potassium dichromate at experimental conditions on a large scale has been achieved at optimum conditions. A quantity of the product was obtained after the evaporation of the solvent by a rotary vacuum evaporator. The precipitate of the product has been collected and dried, then purified by recrystallization in ethanol. To determine the molar extinction coefficient, 0.001 gm of the product which is equivalent to 0.00442mmol dissolved in 10 ml of distilled water, and the absorbance was measured, giving 0.318 at 665 nm, from the Lambert–Beer law(14).

$$A = \varepsilon bc \quad \text{.....(1)}$$

where A is absorbance, C is the concentration (mol/L), b is the thickness of the cell, and ε is the molar extinction coefficient,it was found to be (719.45 L. $mol^{-1}.cm^{-1}$).

Determination of stability constant:

The stability constant for the oxidative coupling reaction of the product was determined according to the equation.

$$k = \frac{[Product]}{[Reactant]} \text{ …….....(2)}$$

Figure 3 shows the UV-vis spectrum of the product at different temperatures after the reaction has been completed. The concentration of the produced amount at each temperature has been established by Beer's Lambert law. The concentrations of the product at different temperatures and the values of the stability constant are listed in Table 2. The results indicate a decrease in the stability constant with increasing temperature, which is attributed to the liberation of protons at higher temperatures (15).

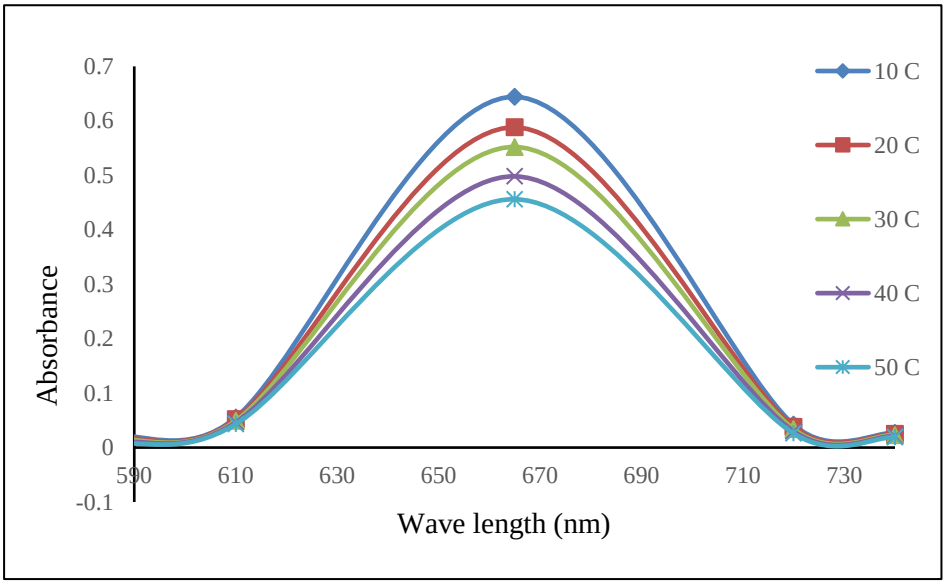

Figure 4: The maximum absorption of the product at λ max at different temperatures

Table 2: The value of maximum absorption for the reaction at different temperatures

Temperature (C^O)	Abs	Conc. mol /L	**K**stability L/mol
10	0.644±0.045	8.95×10^{-1}	20.26
20	0.588±0.012	8.17×10^{-1}	18.50
30	0.552±0.019	7.67×10^{-1}	17.36
40	0.498±0.026	6.90×10^{-1}	15.66
50	0.456±0.024	6.34×10^{-1}	14.35

Kinetic study:

Chemical kinetics is a fundamental subfield of physical chemistry that investigates the reaction rate in each elemental step . It encompasses various aspects such as molecular reaction dynamics, catalytic dynamics, elemental reaction dynamics, micro dynamics, and microdynamics (16). The main objective of chemical kinetics is to analyze the rate of a chemical process and propose the catalytic mechanism using a nonequilibrium dynamic system as the research object, which changes its properties with time. By studying chemical kinetics, we can gain insights into how to control reaction conditions, enhance the main reaction rate, reduce the consumption of raw materials, and improve product quality by suppressing or slowing downside reactions. Chemical kinetics also provides valuable information on how to avoid dangerous goods' explosions, material corrosion, and product aging and deterioration. Nowadays, chemical kinetics has become an essential tool in both chemical discipline development and scientific research. In catalytic reactions, determining the reaction orders can be challenging, as they may not be equal to the stoichiometric number of the chemical reaction in elementary reactions, leading to a complex reaction rate expression and difficulty in identifying the reaction mechanism (17). The rate of reaction may be expressed as follows:

$$R = k\,[A]^x[B]^y \quad \text{………………. (3)}$$

Where R is the rate of reaction, k is the rate constant of reaction, and x and y are the orders of substances A and B, respectively. Given the elementary steps, it is possible to integrate the corresponding rate law to solve for the concentration of some reaction species as a function of time. From equation (3) for the elementary step, the following equations (4, 5, 6, and 7) have been derived and applied to investigate zero, first, and second, respectively.

$$[A_t] = [A_o] - kt \quad \text{………………. (4) (zero order)}$$

$$ln\,\frac{[A_o]}{[A_t]} = k \quad \text{……………..…..…….. (5) (first order)}$$

$$\frac{1}{[A_t]} = \frac{1}{[A_o]} + kt \quad \text{……..…………….(6) (second order)}$$

Effect of phenol concentration

A kinetic spectrophotometric method for rate constant determination of oxidative phenol coupling with 4-amino N, N-dimethylaniline has been described. Different concentrations of phenol at the range (20,40,60,80,100)mg/L with a constant concentration of 4-amino-N, N- dimethylamine 60 mg/L at 25 ^oC were studied. The absorbance at 665 nm was measured at constant time intervals. Equations 4, 5, and 6 were applied to determine the order of reaction and rate constant of the reaction; the results are listed in Table 3. The results indicate that the reaction fellows to first-order reaction as shown in figure 4 from the plot of X=(A_t - A_o) against time and figure 5. From the plot of ln a/ a-x against time with (R^2 = 0.9908 – 0.9926).
The figure below empirical figure that output instrument by directly.

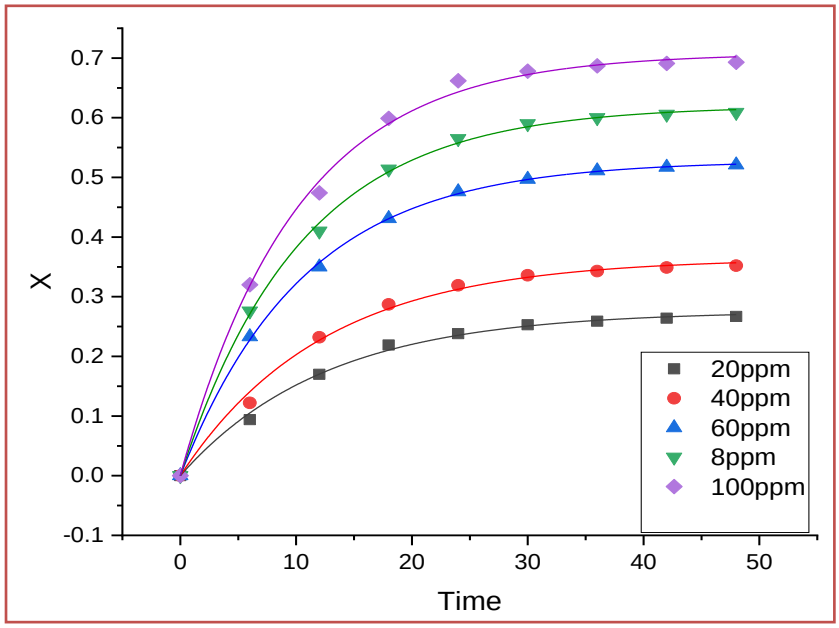

Figure 5: Nonlinear plot X against time for the first-order model at different concentrations and a constant temperature of 30 ºC.

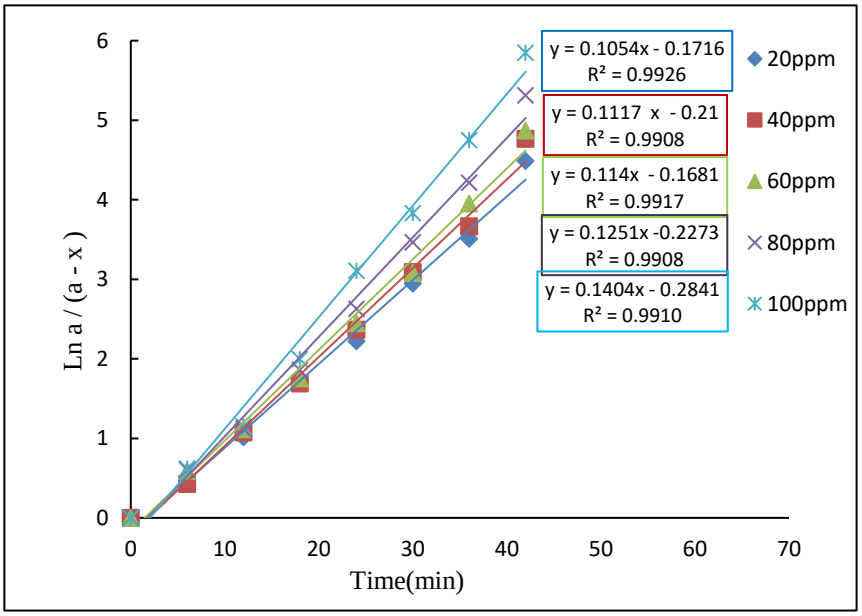

Figure 6: Linear plot Ln a/(a-x) against time for first-order model at different concentrations and constant temperature of 30 ºC.

Effect of temperature

The effect of temperature on the overall order of reaction has been determined by plotting Ln a / (a-x) versus time, as shown in figure 6. The results indicate that the reaction fellows first-order reaction at different temperatures, with the rate of reaction increasing from 0.075 min^{-1} at 10 ºC to 0.23 min^{-1} at 50 ºC. Thus, the increasing rate of reaction with increasing temperature might be due to more molecules colliding, which leads to an increase in the kinetic energy of the molecules and accelerates the reaction to the product. The data of rate constants at different temperatures have been determined for each order and compared according to the correlation coefficient R^2, as listed in Table 3.

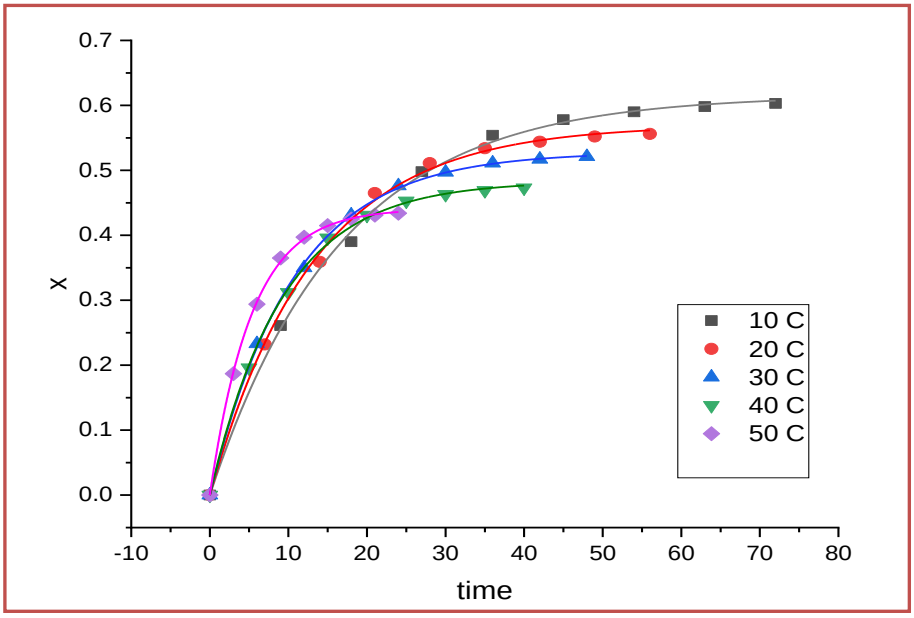

Figure 7: Plot X against time for first-order reaction at different temperatures and constant concentration.

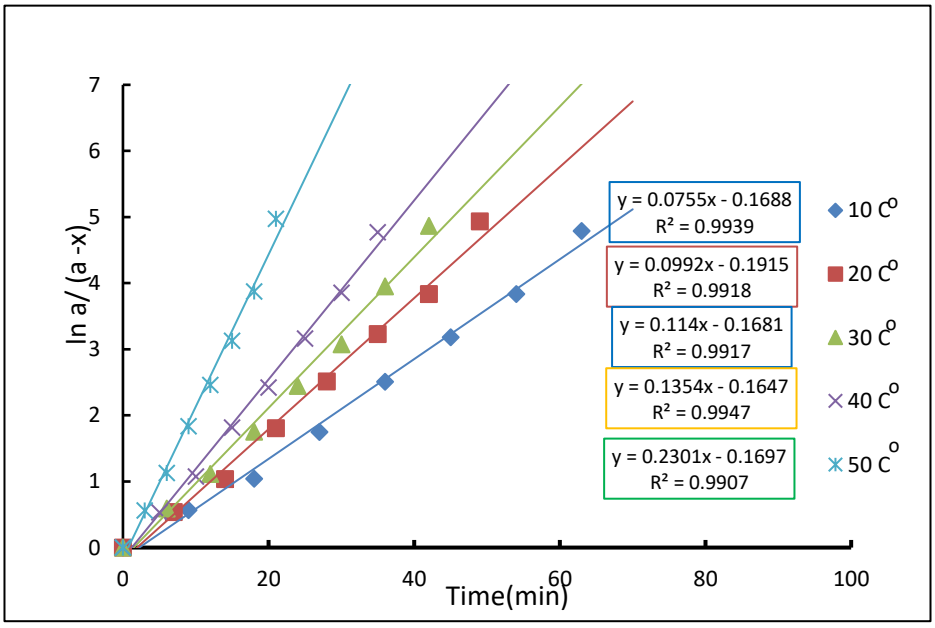

Figure 8: Plot ln a/(a-x) against time for first-order reaction at different temperatures and constant concentration.

Table 3: The values for the linear rate constant at different temperatures for zero-order, first-order, and second-order reactions

Temperature (C^O)	Zero-order		First-order		Second-order	
	Rate constant (mol . L^{-1}.min^{-1})	R^2	Rate constant (min^{-1})	R^2	Rate constant (mol^{-1}. L. min^{-1})	R^2
10	-0.007±0.0005	0.755	0.075±0.007	0.994	2.480±0.09	0.6499
20	-0.008±0.0014	0.754	0.099±0.05	0.982	3.862±0.04	0.615
30	-0.009±0.001	0.746	0.114±0.03	0.992	4.638±0.05	0.636
40	-0.010±0.0019	0.752	0.135±0.08	0.995	5.617±0.03	0.654
50	-0.015±0.0008	0.742	0.17±0.040	0.996	11.91±0.07	0.602

Table 4: The values for nonlinear, the rate constant at different temperatures for first-order reactions

First order				
	Linear		Nonlinear	
Temperature C^O	Rate constant (min^{-1})	R^2	Rate constant (min^{-1})	R^2
10	0.075±0.002	0.994	0.059±0.002	0.998
20	0.099±0.0003	0.982	0.076±0.003	0.998
30	0.114±0.0021	0.992	0.094±0.002	0.999
40	0.135±0.0020	0.995	0.108±0.003	0.999
50	0.171±0.0043	0.996	0.187±0.003	0.995

Thermodynamic parameters of activation

Phenol blue is stable when kept at room temperature. The interaction between enthalpy and entropy changes in chemical reactions is best observed by studying their influence on the equilibrium constants of reversible reactions. The free energy, which is the other thermodynamic parameter, offers a better understanding of the thermodynamic driving factors that shape reactions. An exergonic reaction, which is thermodynamically advantageous and frequently spontaneous, has a negative ΔG*. A positive ΔG* is also indicative of an endergonic response, which needs energy from the environment to proceed (18).

From Arrhenius equation:

$$k = Ae^{-\frac{E_a}{RT}} \quad \text{……..(7)}$$

Where k is the rate constant, Ea is the energy of activation, A is the frequency factor, R is the gas constant, and T is the absolute temperature.

Logarithmic form of the equation .

$$ln\ k = ln\ A - \frac{E_a}{R\ T} \qquad \text{.....(8)}$$

A plot of lnK different 1/T produces a straight line. The gradient, or slope, of the line and its intercept can be used to determine the exponential factor A and the activation energy E_a. The rate constants at different temperatures were determined, and the results are listed in Table 5.

Table 4: The data of rate constants of first-order reaction at different temperature

		Eyring Equation		Arrhenius equation	
Temperature(K)	1/T	The rate constant (k)	ln k/T	The rate constant (k)	ln k
283	0.00353	0.059±0.002	-8.475	0.075±0.002	-2.582
293	0.00341	0.076±0.003	-8.257	0.099±0.0003	-2.310
303	0.0033	0.094±0.002	-8.078	0.114±0.0021	-2.171
313	0.00319	0.108±0.003	-7.971	0.135±0.0020	-2.000
323	0.0031	0.187±0.003	-7.454	0.171±0.0043	-1.772

Application of the Eyring Equation

The linear form of the Eyring Equation is given below:

$$\ln\frac{k}{T} = \frac{-\Delta H^*}{R}\frac{1}{T} + \frac{\Delta S*}{R} + ln\frac{K_B}{h} \qquad \text{.....(9)}$$

The values for ΔH* and ΔS*can be determined from kinetic data obtained from $\ln\frac{k}{T}$ vs. $\frac{1}{T}$ plot. The Equation is a straight line with negative slope, $\frac{-\Delta H^*}{R}$, and a y-intercept, $\frac{\Delta S*}{R} + ln\frac{K_B}{h}$.

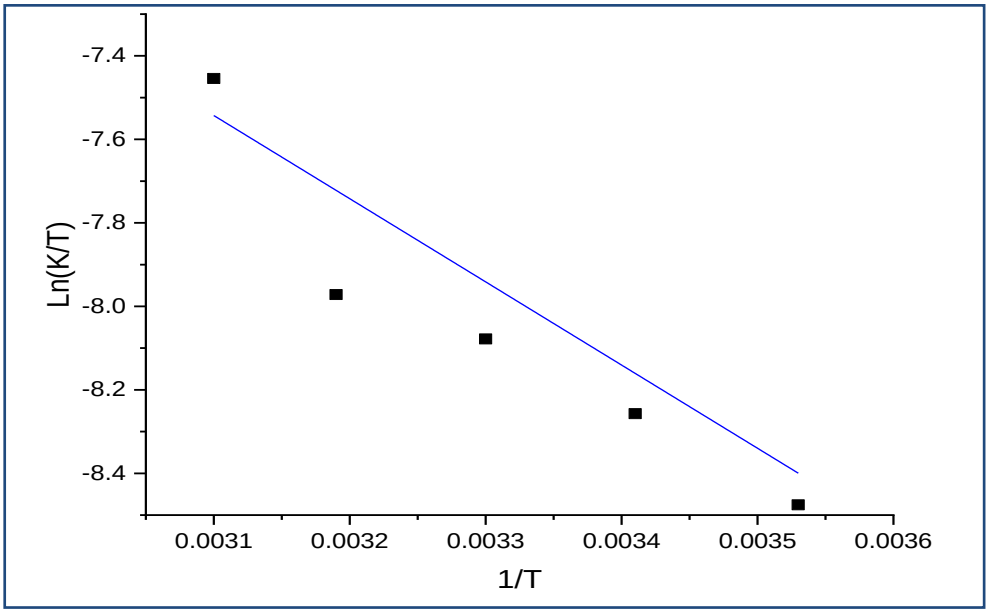

Figure 9: plot of ln(K/T) with 1 /T for the reaction (Erying plot)

$$\Delta G^* = -nRT\ ln\ k_{eq} \qquad \text{.....(10)}$$

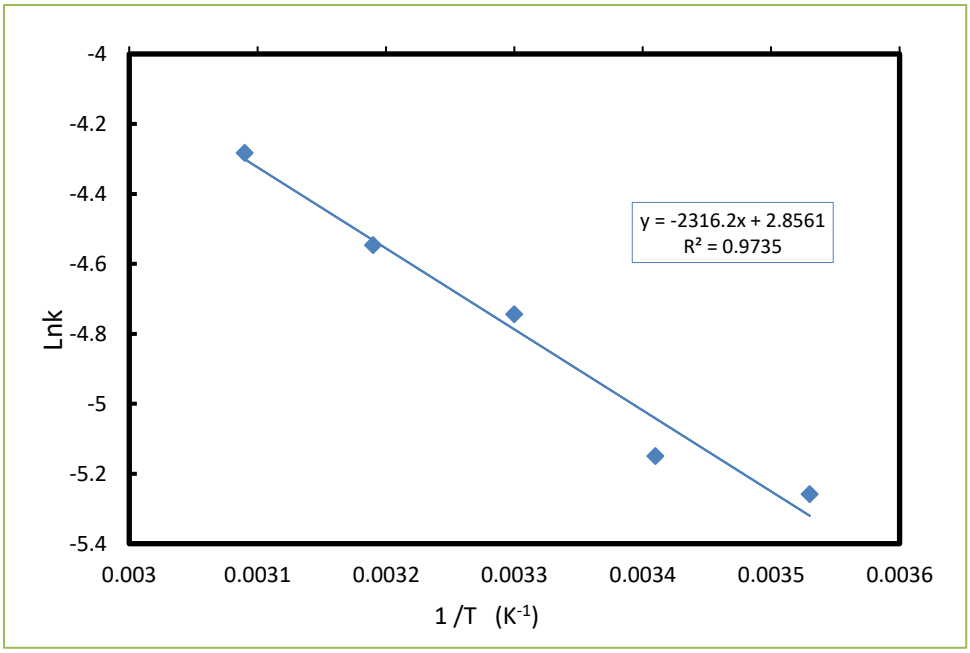

Figure 10: Plot between ln k with 1 /T for the reaction (Arrhenius plot)

The enthalpy (Δ*H**) and entropy (Δ*S**) changes can be calculated by the van't Hoff equation as follows:

$$\Delta G^* = \Delta H^* - T\Delta S^* \quad \text{.....(11)}$$

The equation (11) was used to calculate the data of Gibbs free energy change, ΔG*, against temperature, T. for the oxidative coupling of phenol with 4-amino-N, N-dimethyl amine was obtained. The thermodynamic parameters, including ΔG*, ΔH*, and ΔS*, at different temperatures were calculated and recorded in Table 5. The results indicate that the process is non-spontaneous, as the value of ΔG* decreases with an increase in temperature. Furthermore, the positive value of ΔH* (12.37 Kj/mol) indicates that the reaction is endothermic. The positive value of ΔS*(22.77 $J.mol^{-1}.K^{-1}$) suggests that there is an increased degree of freedom in the system, resulting in the degradation of energy. This positive value of ΔS* also indicates that the system will become more random (19).

Table 5: Data of rate constant, ΔG*, ΔH*, ΔS*, stability constant, and activation energy of the reaction products at different temperature according to Erying equation

Sample	T(K)	Rate constant (min^{-1})×10^{-2}	ΔG* (kj.mol^{-1})	ΔH* (Kj.mol^{-1})	ΔS* (J.mol^{-1})	Kstability (L.mol^{-1})	activation energy (KJ/mol)
phenol	283	0.059±0.002	61.07±0.94			20.25	
	293	0.076±0.003	63.17±1.06			18.50	
	303	0.094±0.002	65.27±1.17	1.640±0.23	210±0.07	17.36	4.16
	313	0.108±0.003	67.37±1.09			15.66	
	323	0.187±0.003	69.47±1.23			14.35	

Table 6: Data of rate constant, ΔG*, ΔH*, ΔS*, stability constant, and activation energy of the reaction products at different temperature according to Arrhenius equation

Sample	T(K)	Rate constant (min^{-1})×10^{-2}	ΔG* ($kj.mol^{-1}$)	ΔH* ($kj.mol^{-1}$)	ΔS* ($j.mol^{-1}$)	Kstability (L. mol^{-1})	activation energy (KJ/mol)
phenol	283	7.55±0.31	6.079±0.201			20.255	
	293	9.92±0.201	5.629±0.203			18.500	
	303	11.4±0.342	5.471±0.121	12.37±0.472	22.77±0.69	17.360	14.89
	313	13.54±0.401	5.203±0.147			15.663	
	323	17.03±0.323	4.754±0.095			14.351	

According to data Arrhenius results are more suitable ,because it is more near from theoretical results.

Dyeing process

The dyeing solution was prepared by dissolve about (0.1-0.2)g alum and 0.1 g of product(phenol blue) in 10 ml disitlled water then the tissues have been immersed on it. The temepratur of the dyeing bath was araized to near 80^{o}C for few minutes. The tissues have been taken out and washed by tap water firstly, then followed by washing with detergents and dried on air. Results show possibility of using the product as dye as in the figure 11 .

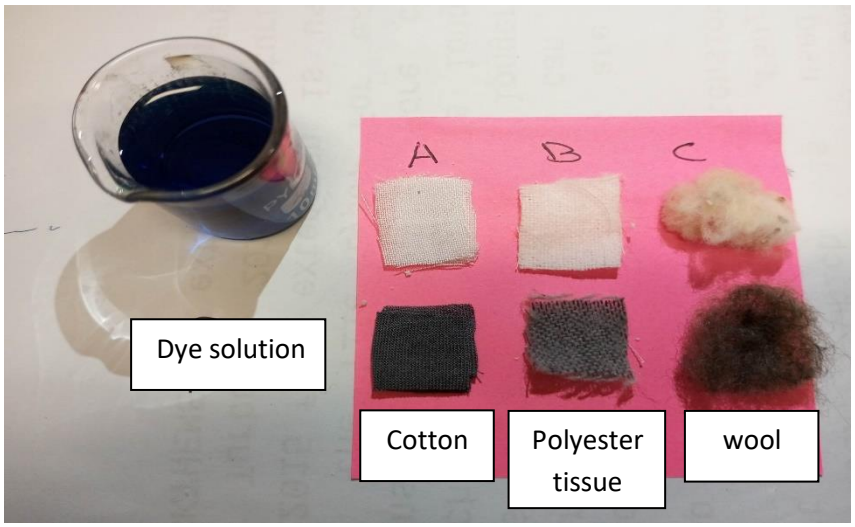

Figure 11: Dyeing of the tissue

Computational study

Computational chemistry is a branch of chemistry that uses computer simulation to assist in solving complex chemical problems. It exploits methods of theoretical chemistry, incorporated into efficient computer programs, to calculate the structures, the interactions, and the properties of molecules .The energy gap between the highest occupied molecular orbit (HOMO) and the lowest vacant molecular orbit (LUMO) is a critical factor that affects the electrical transport characteristics of a molecule (20).In the case of the compound, the energy of the HOMO and LUMO are -52.5945 KJ and -28.9458 KJ, respectively. The energy difference between these orbitals determines the final charge transfer interaction within the molecule, and the frontier orbital energy gap can be calculated using the DFT method and the 6-311G(d,p) basis set, which gives a value

of 23.64 KJ. To calculate the enthalpies and Gibbs free energy of a reaction, one needs to determine the standard heat of the reaction. (21). that involves subtracting the sum of the standard heats of the formation of the reactants from the sum of the standard heats of the formation of the products at a standard temperature of 25℃.

$$\Delta Hr = \sum_{products} \Delta H_f - \sum_{reactants} \Delta H_f \ \ldots\ldots\ldots (1)$$

Given that Gaussian calculates the sum of both electronic and thermal enthalpies, a simpler method to determine the enthalpy of the reaction involves computing the difference between the sums of these values for the reactants and the products. This method is feasible because the number of atoms for each element remains constant on both sides of the reaction, leading to the cancellation of all atomic information (22). Thus, only molecular data is necessary. As an illustration, consider Table 7, which provides information that can be used to compute the enthalpy of the reaction using the following equation:

$$\Delta Hr = \sum_{prod} (\varepsilon_0 + Hcorr) - \sum_{react} (\varepsilon_0 + Hcorr) \ldots\ldots\ldots (2)$$

= ((-726.30304 + -2.3255404) – (-307.35189 + -421.3534))

= 0.07673 x 262.5 = 20.142 KJ/mol.

The same shortcut can be used to calculate Gibbs free energies of reaction

$$\Delta Gr(298K) = \sum_{prod} (\varepsilon_0 + Gcorr) - \sum_{react} (\varepsilon_0 + Gcorr)$$

= (-726.36204 + -2.354978) – (-307.38729 + -421.40215))

= 0.07242 x 262.5 = 19.0099 KJ/mol

Table 7: Calculated thermochemistry values from Gaussian for the reaction (All values are in Hartree Unit = 2625.5 kJ/mol).

	Sample	Reagent	Product	$2H_2$
Ɛ0 + Ɛ ZPE	-307.358312	-421.365110	-726.318947	-2.332014
Ɛ0 + Etot	-307.352835	-421.354344	-726.303980	-2.327292
Ɛ0 + H Corr	-307.351891	-421.353400	-726.303036	-2.3255404
Ɛ0 + G Corr	-307.387290	-421.402145	-726.362038	-2.354978

Where Ɛ0 + Ɛ ZPE is the sum of electronic and zero-point Energies , Ɛ0 + Etot is sum of electronic and thermal Energies, Ɛ0 + H Corr is sum of electronic and thermal Enthalpies, Ɛ0 + G Corr is sum of electronic and thermal Free Energies.

In Figure 9, the calculated energies of the highest occupied molecular orbital (HOMO) and lowest unoccupied molecular orbital (LUMO) are displayed. All the calculations in this research were performed using the Gaussian 09 program (23,24). The molecular orbital energy gap was investigated as it is crucial to determine the kinetic stability of the compounds. At 298K, Table (8) presents the stability constant, $E_{(LUMO)}$, $E_{(HOMO)}$, and molecular orbital energy gap of the product. The stability constant of the complex was determined by calculating the corresponding Gibbs free energy of the reaction, ΔGr. A large HOMO-LUMO gap indicates high kinetic stability and low chemical reactivity since it is energetically challenging to add electrons to a high-lying LUMO. On the other hand, a soft molecule has a small frontier orbital gap, is more polarizable, often exhibits high chemical reactivity, and has low kinetic stability (25).

Table 8: The theoretical value of stability constant, activation energy, enthalpy, free energy, entropy EHOMO, ELUMO, and Egap for the product of the reaction between phenol with 4-amino-N, N-dimethylaniline at 298K.

parameter	Kstability L/mmol) 10^{-3}	Ea* (kJ.mol^{-1})	ΔH* (KJ.mol^{-1})	ΔG* (KJ.mol^{-1})	ΔS* (J.mol^{-1})	E_{HOMO} (KJ.mol^{-1})	E_{LUMO} (KJ.mol^{-1})	Egap (KJ.mol^{-1})
Theoretical	21.57	22.62	20.15	19.1	40.15	-52.5945	-28.94	23.65
Practical Arrhiuns equation	17.360	14.89	12.37 ±0.472	5.471 ±0.121	22.77 ±0.69			
Practical Eyring equation	17.36	4.16 ±0.24	1.64 ±0.234	65.27 ±1.17	210 ±9.07			

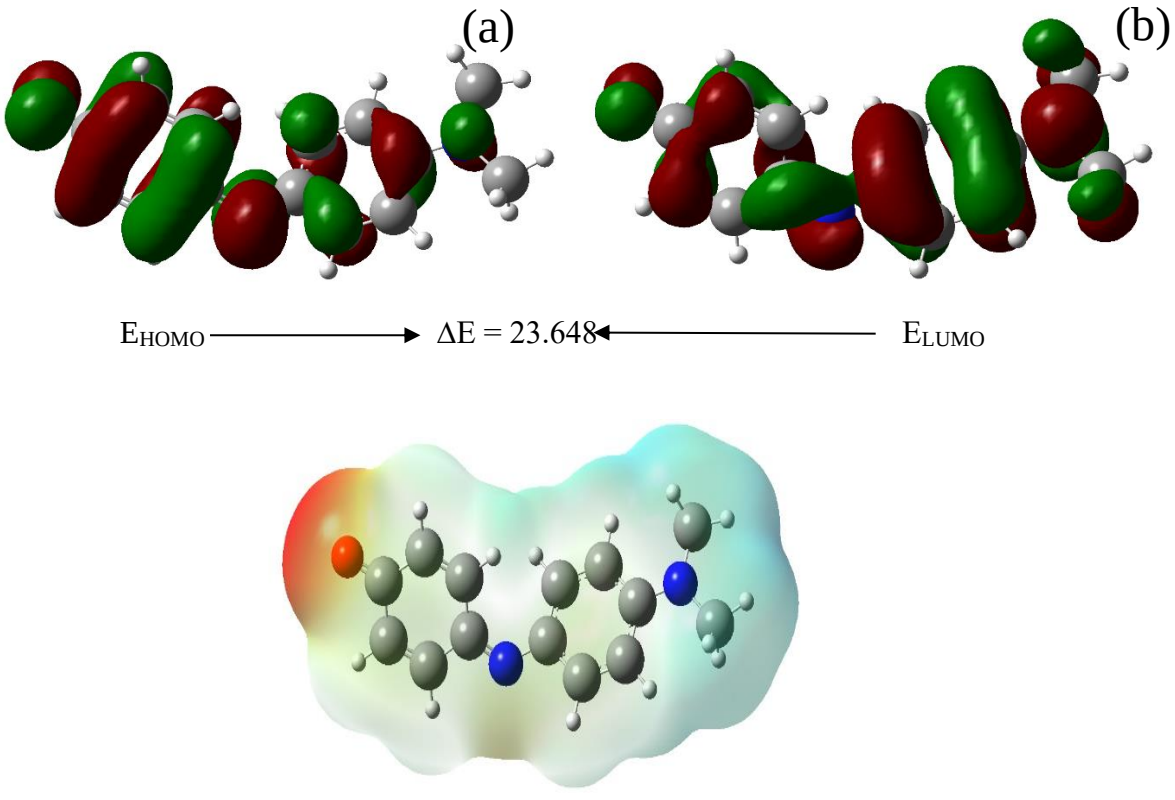

Figure 12: Frontier molecular orbital of phenol blue (a) The highly occupied molecular orbitals (HOMO), (b) lowest unoccupied molecular orbitals (LUMO) and (c) electro static maps of the product.

DFT (Density Functional Theory) calculated data is obtained through computational methods, while practical data is obtained through experiments. DFT calculations are faster than practical experiments (26).

The optimized molecular geometry, vibrational frequencies, infrared activities, energy gap between HOMO-LUMO, and thermodynamics of the molecule in the ground state have been calculated by using DFT (B3LYP) methods with a 6–31+G (d, p) basis set. The vibrational frequencies were calculated and scaled values are compared with the recorded IR spectra of the compound. The observed and calculated frequencies are found to be in good agreement. Furthermore, the thermodynamic and total dipole moment properties of the compound have been calculated to get insight into the molecular structure of the compound. These computations are carried out with the main aim that the results will be of assistance in the quest for experimental and theoretical evidence for the title molecule in biological activity and coordination chemistry (27).

In another article, the theoretical aspects of the thermodynamic calculation of the Gibbs energy and heat capacity of a crystalline system within the frame of the Density Functional Theory (DFT) are introduced in the present chapter. Various approximations of phonon motion (harmonic, quasiharmonic, and anharmonic) and their effects on the thermodynamic properties are discussed. The theoretical basis of the thermodynamic approach to the heat capacity of crystals for given thermodynamic conditions is presented, having as an example six polymorphs of the magnesium hydrides (28).

The optimized geometry, wavenumber, polarizability, and several thermodynamic properties of dacarbazine were studied using ab initio Hartree-Fock, MP2, and DFT methods. A complete vibrational assignment aided by the theoretical harmonic wavenumber analysis was proposed. The calculated harmonic vibrational frequencies were compared with experimental FTIR and FT Raman spectra. Based on the comparison between calculated and experimental results and the comparison with related molecules, assignments of fundamental vibrational modes were made. The X-ray geometry and experimental frequencies were compared with the results of theoretical calculations (29).

DFT has several advantages over theoretical data. DFT allows the calculation of the equilibrium particle density and prediction of thermodynamic properties and behavior of a many-body system on the atomic scale. DFT calculations can be used to determine the heat of formation and the energetic density of compounds (30).

Conclusions

The oxidative coupling reaction of phenol has proven to have extensive applications in various fields, including pharmaceuticals, agriculture, industry, and environmental analysis. In this study, blue phenol was synthesized by oxidatively coupling phenol with 4-amino-N, N-dimethyl aniline in the presence of potassium dichromate in an alkaline medium. The stability constant and kinetics of the product were determine using spectrophotometry, revealing a first-order reaction. Additionally, the effects of temperature were investigated, and thermodynamic parameters such as free Gibbs energy, enthalpy, and entropy were determined. It was found that the formation of phenol blue was non-spontaneous and endothermic. Furthermore, using DFT computations with the common 6-311G(d,p) basis set, Gaussian thermochemistry was employed to calculate the enthalpy, Gibbs free energy and entropy change (of activation) heat of molecule formation, and absolute reaction rates of the phenol oxidative reaction. These results provide valuable insight into the properties of the reaction and its potential applications.

Conflict of interest

The authors confirm that they are not affiliated with or involved in any organization or entity with financial interests.

Acknowledgments

This research was supported by the University of Sulaimani. We thank the College of Science and Department of Chemistry of Sulaimani University for their support. I would like to express my great thanks to the Ministry of Education for allowing us to continue with our aims. We thank all staff of chemistry department that supports the OriginLab Programme.

References

1. Funes-Ardoiz I, Maseras F. (2018). Oxidative coupling mechanisms: current state of understanding. ACS Catalysis. Feb 2;8(2):1161-72.
2. Son YW, Kwon TH, Lee JK, Pae AN, Lee JY, Cho YS, Min SJ. (2011). A concise synthesis of tetrabenazine: an intramolecular aza-Prins-type cyclization via oxidative C–H activation. Organic Letters. Dec 16;13(24):6500-3.
3. Wu J, Kozlowski MC. (2022). Catalytic oxidative coupling of phenols and related compounds. ACS catalysis. May 18;12(11):6532-49.
4. Sarhan AA, Bolm C. (2009). Iron (III) chloride in oxidative C–C coupling reactions. Chemical Society Reviews. 38(9):2730-44.
5. Marino JP, Schwartz A. (1979). Selective catechol oxidations with diphenyl selenoxide. Applications to phenolic coupling. Tetrahedron Letters. Jan 1;20(35):3253-6.
6. Syrjänen K, Brunow G. (1998). Oxidative cross-coupling of p-hydroxycinnamic alcohols with dimeric arylglycerol β-aryl ether lignin model compounds. The effect of oxidation potentials. Journal of the Chemical Society, Perkin Transactions 1. (20):3425-30.
7. Vershinin V, Forkosh H, Ben-Lulu M, Libman A, Pappo D. (2020). Mechanistic insights into the FeCl3-catalyzed oxidative cross-coupling of phenols with 2-aminonaphthalenes. The Journal of Organic Chemistry. Dec 9;86(1):79-90.
8. Paniak TJ, Kozlowski MC. (2020). Aerobic Catalyzed Oxidative Cross-Coupling of N, N-Disubstituted Anilines and Aminonaphthalenes with Phenols and Naphthols. Organic letters. Feb 12;22(5):1765-70.
9. Casellato U, Tamburini S, Vigato PA, Vidali M, Fenton DE. (1984). Binuclear oxovanadium (IV) complexes as catalyst for the oxygenation of the catechols. Inorganica chimica acta. Apr 16;84(1):101-4.
10. Edwards W, Leukes WD, Rose PD, Burton SG. (1999). Immobilization of polyphenol oxidase on chitosan-coated polysulphone capillary membranes for improved phenolic effluent bioremediation. Enzyme and microbial technology. Nov 1;25(8-9):769-73.
11. Yamada K, Akiba Y, Shibuya T, Kashiwada A, Matsuda K, Hirata M. (2005). Water purification through bioconversion of phenol compounds by tyrosinase and chemical adsorption by chitosan beads. Biotechnology progress. 21(3):823-9.
12. Ashour S. (2013). New kinetic spectrophotometric method for determination of atorvastatin in pure and pharmaceutical dosage forms. Pharmaceutica Analytica Acta. 4(5):1-6.
13. Brooker LG, Sprague RH. (1941). Color and constitution. IV. 1 The absorption of phenol blue. Journal of the American Chemical Society. Nov;63(11):3214-5.
14. Kumar A, Singh S, Mudahar GS, Thind KS. (2006). Molar extinction coefficients of some commonly used solvents. Radiation Physics and Chemistry. Jul 1;75(7):737-40.
15. Thakur SV, Farooqui M, Naikwade SD. (2012). Thermodynamic studies of transition metal complexes with Metformin Hydrochloride drug in 20%(v/v) ethanol-water mixture. Der Chemica Sinica. 3(6):1406-9.

16. Murzin DY. (2020). Requiem for the rate-determining step in complex heterogeneous catalytic reactions?. Reactions. Sep 10;1(1):4.
17. Schmidt OP, Dechert-Schmitt AM, Garnsey MR, Wisniewska HM, Blackmond DG. (2019). Kinetic analysis of catalytic organic reactions using a temperature scanning protocol. ChemCatChem. Aug 21;11(16):3808-13.
18. Schmidt OP, Dechert-Schmitt AM, Garnsey MR, Wisniewska HM, Blackmond DG. (2019). Kinetic analysis of catalytic organic reactions using a temperature scanning protocol. ChemCatChem. Aug 21;11(16):3808-13.
19. Fabian Huxoll, Anna Kampwerth, Thomas Seidensticker, Dieter Vogt, Gabriele Sadowski, (2022) " predicting solvent effects on homogeneity and kinetics of the hydro amino methylation: A thermodynamic approach using PC-SAFT" Ind. Eng. Chem. Res. 61,5, 2323- 2332.
20. Pereira F, Xiao K, Latino DA, Wu C, Zhang Q, Aires-de-Sousa J. (2017)Machine learning methods to predict density functional theory B3LYP energies of HOMO and LUMO orbitals. Journal of chemical information and modeling. Jan 23;57(1):11-21.
21. Tanış E. (2022). New optoelectronic material based on biguanide for orange and yellow organic light emitting diode: A combined experimental and theoretical study. Journal of Molecular Liquids. Jul 15;358:119161.
22. Jaramillo P, Domingo LR, Chamorro E, Pérez P. A (2008). further exploration of a nucleophilicity index based on the gas-phase ionization potentials. Journal of Molecular Structure: THEOCHEM. Sep 30;865(1-3):68-72.
23. Deuri S, Phukan P. (2012). A DFT study on nucleophilicity and site selectivity of nitrogen nucleophiles. Computational and Theoretical Chemistry. Jan 15;980:49-55.
24. Tanış E. (2022). New optoelectronic material based on biguanide for orange and yellow organic light emitting diode: A combined experimental and theoretical study. Journal of Molecular Liquids. Jul 15;358:119161.
25. Udhayakala P, Rajendiran TV, Seshadri S, Gunasekaran S. (2011). Quantum chemical vibrational study, molecular property and HOMO-LUMO energies of 3-bromoacetophenone for Pharmaceutical application. J. Chem. Pharm. Res. 3(3):610-25.
26. Mazurek AH, Szeleszczuk Ł, Pisklak DM. (2020). Periodic DFT calculations—review of applications in the pharmaceutical sciences. Pharmaceutics. May 1;12(5):415.
27. Ayalew ME. (2022). DFT Studies on Molecular Structure, Thermodynamics Parameters, HOMO-LUMO and Spectral Analysis of Pharmaceuticals Compound Quinoline (Benzo [b] Pyridine). Journal of Biophysical Chemistry. Aug 19;13(3):29-42.
28. Chihaia V, Alexiev V, AlMatrouk HS. (2022). Assessment of the Heat Capacity by Thermodynamic Approach Based on Density Functional Theory Calculations. Applications of Calorimetry. Jun 23:41.
29. Gunasekaran S, Kumaresan S, Arunbalaji R, Anand G, Srinivasan S. (2008). Density functional theory study of vibrational spectra, and assignment of fundamental modes of dacarbazine. Journal of Chemical Sciences. May;120:315-24.
30. Chugunova E, Shaekhov T, Khamatgalimov A, Gorshkov V, Burilov A. (2022). DFT Quantum-Chemical Calculation of Thermodynamic Parameters and DSC Measurement of Thermostability of Novel Benzofuroxan Derivatives Containing Triazidoisobutyl Fragments. International Journal of Molecular Sciences. Jan 27;23(3):1471.